Kwon and Kim *Fash Text* (2021) 8:27
https://doi.org/10.1186/s40691-021-00251-y

Fashion and Textiles

REVIEW Open Access

Performance of wearables and the effect of user behavior in additive manufacturing process

JuYoun Kwon[1] and Namhun Kim[2*]

*Correspondence:
nhkim@unist.ac.kr
[2] Department of Mechanical Engineering, Ulsan National Institute of Science and Technology, Ulsan, Korea
Full list of author information is available at the end of the article

Abstract

Additive manufacturing (AM) which can be a suitable technology to personalize wearables is ideal for adjusting the range of part performance such as mechanical properties if high performance is not required. However, the AM process parameter can impact overall durability and reliability of the part. In this instance, user behavior can play an essential role in performance of wearables through the settings of AM process parameter. This review discusses parameters of AM processes influenced by user behavior with respect to performance required to fabricate AM wearables. Many studies on AM are performed regardless of the process parameters or are limited to certain parameters. Therefore, it is necessary to examine how the main parameters considered in the AM process affect performance of wearables. The overall aims of this review are to achieve a greater understanding of each AM process parameter affecting performance of AM wearables and to provide requisites for the desired performance including the practice of sustainable user behavior in AM fabrication. It is discussed that AM wearables with various performance are fabricated when the user sets the parameters. In particular, we emphasize that it is necessary to develop a qualified procedure and to build a database of each AM machine about part performance to minimize the effect of user behavior.

Keywords: 3D printing, Additive manufacturing, User behavior, Wearable device, Process parameters, Mechanical properties

Introduction

Additive manufacturing (AM) is well-known as technology to fabricate customized consumer goods (Kwon et al. 2017). Specifically, AM can be a suitable technology to customize wearables and AM has been applied to the wearable industry, a high value-added business because functionality, arising from various anthropometric dimensions and a range of different human needs, can be materialized. For example, personalized running shoes are developed by AM (Silbert 2019), and the world record was broken by a marathoner wearing ultralight weight footwear (Burfoot 2019). The wearables worn by human would demand tensile and tear strength, a high degree of flexibility, low density, and strong resistance to moisture and chemicals, considering human characteristics. The pressure of human tissue ranges from 1 to 500 kPa when considering body movements

by humans ranging from a finger touch to standing posture (Yeo & Lim 2016). AM can materialize the characteristics by adjusting the degree of part performance such as mechanical properties if high performance is not required (Croccolo et al. 2013). However, the unexpected attenuation of performance is caused by the change of mesostructure and anisotropy affected by the AM process parameter (Es-Said et al. 2000). When fabricating AM wearables, thus, the AM process parameter can impact the overall durability and reliability of the part. In this instance, a human adjusts AM process parameters and subsequent human behavior can play a crucial role in the performance.

Furthermore, user behavior in the AM process also affects its environmental impact. A few industries believe AM can reduce the effect of user behavior (Schrank & Stanhope 2011; Valtas & Sun 2016) but the actual resource waste caused by machine or user behavior would be larger than expectations (Song & Telenko 2016). Notably, users whose lack experience in AM induce part failure, and environmental impact can increase by 26.3%, when caused by material and power waste (Song & Telenko 2019). They suggested that human and organizational behavior may alter the failure rate. A study (Liu et al. 2019) presents a framework of designs for additive manufacturing (DfAM) on the basis of users, who have vocational experiences in AM, and it shows the short life cycle of AM parts and its negative effect on the environment due to resource waste. Besides, a worksheet to screen 3D CAD models before printing can help decrease failures by 80% (Booth et al. 2017). These previous studies present the effect of human behavior on the preprocess and inprocess stages of AM (Fig. 1).

AM technology demands the reliability of successful builds, the improvement of production yield, and the time reduction for postprocess and material consumption stages (DNV GL 2017) and these demands can be achieved by the combination of the preprocess, inprocess, and postprocess stages. User behavior is implicated in these processes in obtaining the proper performance of wearables as well as a lower environmental impact. However, both the understanding of AM process parameters related to user behavior and the efforts arising from the trial-and-error process decrease are essential to the low environmental impact of the AM process (Fig. 2), but a discrepancy exists between human practice and attitudes toward the environment (Kollmuss & Agyeman 2002). For instance, the AM parts which do not conform to the customers' requirements are just thrown away without considering recycling (Liu et al. 2019). Moreover, many studies on AM are performed regardless of the process parameters (Yao et al. 2017) or are limited to certain parameters such as part orientation (Zehtaban et al. 2016) and layer thickness

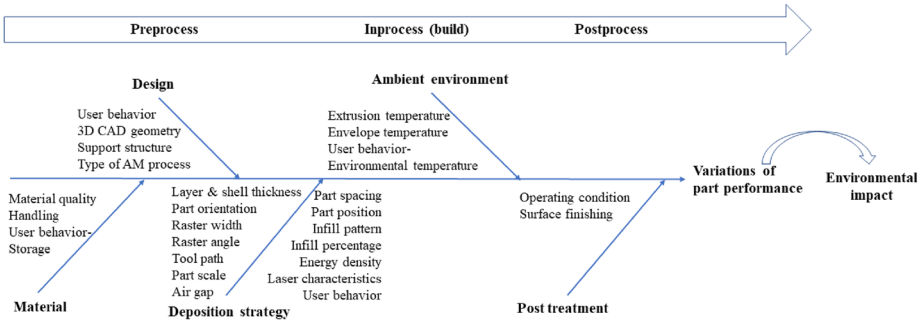

Fig. 1 AM process, and its most influential parameters on performance involved by users

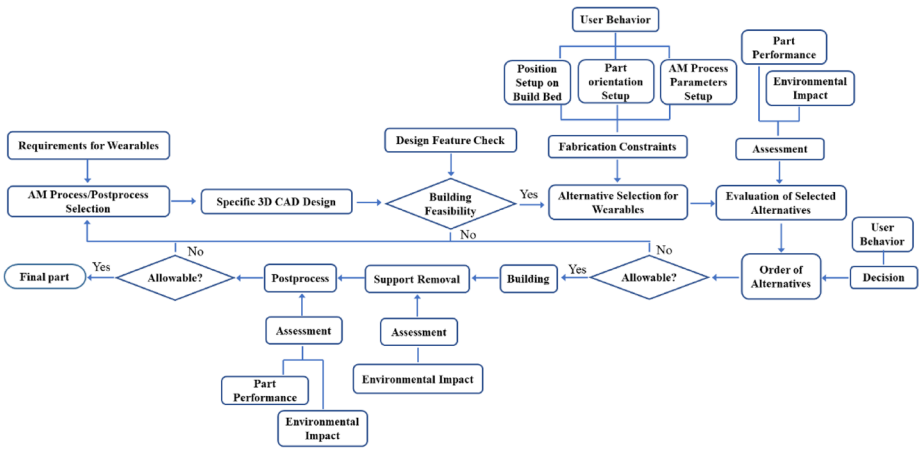

Fig. 2 Logistics practice for the AM process, in consideration of performance and user behavior for AM wearables fabrication

(Vidakis et al. 2017). Because fabrication inaccuracy often occurs during actual product manufacturing, a technology that can automatically inspect the product is used (Tseng et al. 2014). Therefore, it is necessary to examine how the main parameters considered in the AM process affect the performance. The overall aims of this review are to achieve a greater understanding of each AM deposition parameter affecting the performance of AM wearables and to provide requisites for the desired performance in the AM fabrication including the practice of sustainable user behavior. This review discusses AM process parameters which affect performance of AM wearables (Table 1) and AM processes which are often used for wearables fabrication: namely, material extrusion, material jetting, vat photopolymerization, and powder bed fusion processes. Performance in this review means surface topography as well as geometric and mechanical properties caused by the AM process parameter.

This article is organized as follows. The four types of AM processes which are often used for wearables fabrication are discussed. The research trends of AM wearables on performance are also examined. After that, parameters related to user behavior are described with a focus on the effect on performance which consists of surface, geometric and mechanical properties. Then the wearables studies are discussed on AM fabrication cases with AM process parameters and requisites for the fabrication of AM wearables with desired performance are examined.

AM process parameters

Each AM process requires specific parameters, but AM-using polymers exhibits the parameters of some typical processes (AMSC 2017) which are discussed in this section. The state of material also affects surface quality and deformation which may result in the requirement of a postprocess stage (Xu et al. 1999). Therefore, AM parts should be designed to consider the characteristics of AM processes. Especially, wearables are ordinarily fabricated by the AM processes (Banga et al. 2018; Davia-Aracil et al. 2018; Guerra et al. 2018) which are as follows: material extrusion, material jetting, vat photopolymerization, powder bed fusion processes. This section discusses the characteristics of the

Table 1 Performance investigated by previous studies about AM wearables

Wearables applications	AM processes/material	Surface topography	Geometric properties	Stiffness	Compressive behavior	Flexural properties	Impact energy	Elongation at break	Hardness	Ref.
PPE[a]	Material extrusion/TPU[c]						v			Bates et al. (2016)
PPE[a]	Material extrusion/nylon				v					Rossiter et al. (2020)
Wrist splint	Powder bed fusion/nylon Material extrusion/ABS[d] Vat polymerization/ABS[d] Material jetting/ABS[d]	v	v							Paterson et al. (2015)
Bicycle helmet	Powder bed fusion/TPE[e], Duraform			v	v			V		Soe et al. (2015)
Stab-resistant amour	Powder bed fusion/Duraform						v			Johnson et al. (2013)
Insole	Material extrusion/TPU[c]						v			Davia-Aracil et al. (2018)
AFO[b]	Material extrusion/ABS[d]			v			v			Aydin and Kucuk (2018)
AFO[b]	Powder bed fusion/nylon			v						Ielapi et al. (2019)
AFO[b]	Material extrusion/polyurethane		v							Cha et al. (2017)
AFO[b]	Material extrusion/TPU[c], PLA[f] composite			v				V		Tao et al. (2019)
Shin pads	Material jetting/rubber-like material					v	v			Cazon-Martin et al. (2018)
AFO[b]	Powder bed fusion/nylon			v						Deckers et al. (2018)
AFO[b]	Powder bed fusion/nylon			v						Telfer et al. (2012)
PPE[a]	Powder bed fusion/nylon				v					Brennan-Craddock et al. (2008)
AFO[b]	Material extrusion/PLA			v						Choi et al. (2017)
Wrist orthosis	Material extrusion/ABS			v		v				Palousek et al. (2014)
Hinge joint	Material jetting/rubber-like	v								Meisel et al. (2015)
Insole	Material extrusion/TPU			v		v			v	Yarwindran et al. (2016)
AFO[b]	Powder bed fusion		v			v				Schrank and Stanhope (2011)

[a] PPE means personal protective equipment

[b] AFO means ankle foot orthoses

[c] TPU means thermoplastic polyurethane

[d] ABS means acrylonitrile butadiene styrene

[e] TPE means thermoplastic elastomer

[f] PLA means polylactic acid

four AM processes and their typical parameters. Concrete directions relating to orientation in this article follow ISO/ASTM 52921 (Fig. 3) (ISO/ASTM 52921 2016).

Material extrusion process

Fused deposition modelling (FDM) is one of the material extrusion processes, and thermoplastic materials made of solid filaments which are extruded through the nozzle are used by building them up layer-by-layer. Support is printed along the bottom of the part, and manual work and auxiliary equipment utilizing soluble detergent are required for support removal (Kwon et al. 2020). Various process parameters manipulated by users are involved: layer thickness, part orientation, raster angle, raster width, infill pattern, air gap, tool path generation, etc. (Fig. 1) (Mohan et al. 2017). In addition, shell thickness (Lanzotti et al. 2015) and support structure (Jin et al. 2016) affect ultimate tensile strength and dimensional accuracy. Particularly, various parameters in the preprocess stage play an important role in dimensional accuracy, surface roughness, build time, and other mechanical properties (Chohan et al. 2016) and flow rate, extrusion, envelope and environmental temperatures are considered parameters in the inprocess stage (Bahr & Westkamper 2018). Generally, an appropriate extrusion temperature can be set if material loaded on the machine is identical to the material selected via the software. Some AM systems do not require material selection, but others require that users should manually select the material using the software. In addition, envelope temperature is easily influenced by environmental conditions if the machine does not have the functionality to heat the chamber. Ultimately, how users determine these parameters affects performance of wearables. For example, FDM has superb impact strength (Kim & Oh 2008) but the part orientation can reduce the tensile and impact strengths. Meanwhile, the combination of part orientation and tool-path generation can decrease support structure for fabricating FDM wearables without compromising strength (Jin et al. 2016). Besides, filament materials can have high porosity which induce poor surface quality in final parts (Barbero 2011), and postprocessing to get rid of the pores is often demanded. However, structures with porosity can be desirable for certain purposes such as for use in wearables. Structures with porosity can be utilized for wearable health care devices involved in biofluid transportation.

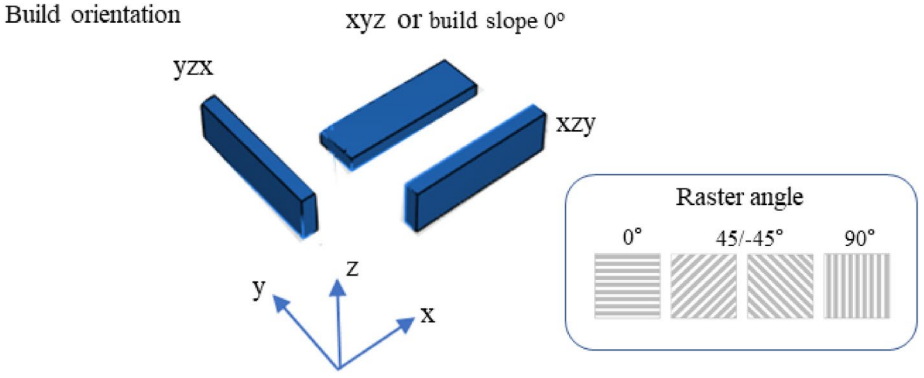

Fig. 3 Raster angle and part orientation, which means build orientation and slope. *Build orientation xyz, xzy, and yzx followed by ISO/ASTM standard

Material jetting process

Photopolymer jetting (PJ) represents one of the material jetting processes, and photopolymer resins for objects and support are used to deposit an object in layer-by-layer. The materials, shoot on the build bed, are exposed to UV lamps for vulcanization. Users setup part orientation and AM preprocess parameters on GrabCad software; tray materials, surface finish, grid style, etc. (GrabCad 2019). There combination makes variation of performance, material consumption and build time, which conclusionally affects electricity (Das et al. 2018). Especially, the influences of PJ on the environment are larger than those of other AM processes (Kwon et al. 2020). In addition, the part position on the build bed can affect mechanical properties because the UV exposure of PJ affects mechanical properties (Barclift & Williams 2012).

Vat photopolymerization process

Stereolithography (SL) represents one of the vat photopolymerization processes. A laser beam shoots photopolymer resin in a tank for part consolidation. SL has good hardness, surface roughness, and dimensional accuracy (Kim & Oh 2008). However, SL has a limitation in terms of using multi-materials in rapid build time although SL is advantageous in build time, resolution, and complex geometry. The single-resin system will evolve through improvement of material chemistries (Wallin et al. 2018). Research showed that there was not much difference in gait analysis between size-customized SL wearables and manually fabricated ones (Mavroidis et al. 2011). Meanwhile, the 3D geometries of wearables should be designed carefully, considering that the resin can be trapped in the internal parts. Trapped volume in the SL process causes damages within the parts, while in the Laser sintering (LS) process it distorted the part (Ang et al. 2000).

Powder bed fusion process

LS represents one of the powder bed fusion processes. Powder-type thermoplastic materials is used, and a CO_2 laser beam is shot on the powder of the build bed. The powder on the bed plays a role in terms of support, and the remaining powder, which can be recycled, is separated from the fabricated part. LS presents good compressive strength and rapid build time (Kim & Oh 2008) and enables serial production. Depending on the manufacturers, users can control different parameters of machines; layer thickness, build bed temperature, removal chamber temperature, laser power, scan speed, scan spacing, and preheat time (Majewski & Hopkinson 2011). For instance, laser power, scan speed, scan spacing, bed temperature, and scan length are considered when improving the accuracy of a shrinkage rate model (Mavroidis et al. 2011) and part orientation affects dimensional accuracy of wearables such as an ankle–foot orthosis (AFO) (Croccolo et al. 2013). In addition, performance of wearables is influenced by the condition of material storage as well as the characteristics of powder; humidity in the material, particle size and shape, and fresh and recycled powder (Bahr & Westkamper 2018; Raghunath & Pandey 2007). Particularly, an additional process can be required depending on the geometries if remaining powder is trapped in an internal part. Therefore, the 3D CAD model should be designed in consideration of this aspect of LS (Scharff et al. 2017).

Performance considered when fabricating AM wearables

AM has been applied to develop electromechanical devices including stretchable e-skin film with a net-shaped structure, and environment monitoring (FDA 1997; Paterson et al. 2015). Wearables have been developed to detect, for example, hydrogen peroxide and glucose (Comina et al. 2014), utilize smart materials to monitor human physiological responses (Kwon et al. 2017), and perform energy-efficient locomotion by manipulating the gradient of soft and hard components (Wallin et al. 2018).

AM can also be applied to customize personal protective equipment (PPE). At this time, DfAM can be utilized to develop effective and easy-to-use PPE. Human skin continues to breathe even during sleep and evaporates sweat from the skin. Wearables worn by humans can increase comfort by using DfAM to improve permeability even when sweating. The sports PPE a shock absorber of strut structure was developed for body protection (Table 1) [e.g. shin pads with lattice structure for football players (Cazon-Martin et al. 2019), and insoles with shock absorption, flexibility, etc. (Davia-Aracil et al. 2018)].

Furthermore, functional compositions such as designs and arrays of various AM textiles can be developed, considering the movement of wearers (Johnson et al. 2013). FDM and SL are often used for the development of medical devices using polylactic acid (PLA) (Miclaus et al. 2017) and PJ is used for the development of assistive devices (Davia-Aracil et al. 2018). Table 1 represents the performance considered by studies on AM wearables and surface quality, geometric properties and mechanical properties were investigated for performance of AM wearables. The next section discusses AM process parameters which affect those performance in preprocess, inprocess and postprocess stages.

Influential AM process parameter on performance of wearables

The desired performance for the requirements of wearables is very important for guaranteeing cost effectiveness and product reliability (Wang et al. 1996), and performance is affected by AM process parameters including postprocess and material characteristics (AMSC 2017). In this stage, user behavior plays an essential role in performance through the setting of parameters (Fig. 2) and it is valuable to identify parameters of AM processes determined by user behavior. Therefore, this section reviews the influence of each AM process parameter on surface, geometric and mechanical properties of AM parts.

Influence of AM process parameters on surface topography

The surface topography of the AM process has a stairstepping effect, but it is the main concern of some industries in AM parts. The surface topography can be affected by AM process parameters which are setup by users, so it is valuable to identify the characteristics of parameters. Layer thickness is the most prominent parameter for surface roughness, compared with build speed and raster width, and it has an inverse relation with surface roughness. Meanwhile, the thin layer thickness causes slow build time (Huang et al. 2019, Table 2). Therefore, users can make the decision of slow build time if the importance to surface quality is assigned. However, the build time is directly related to the electricity used, which affects its environmental impact. Additionally, the layer thickness of FDM causes lower resolution than that of other AM processes such as SL, LS, and PJ (Kim et al. 2018).

Table 2 Influential AM parameters on surface topography

AM process / material	Layer thickness (mm)	Raster angle	Part orientation/ surfaces inclination	Postprocess stage	Material quality	Roughness (μm)			Ref.
FDM/ABS[a]	0.1	45/− 45	Horizontal		Filament dried in vacuo for 4 h at 80 °C	6.4–20.4			Huang et al. (2019)
	0.2	30/− 60	Lateral			Difference between max and min: 7 for layer thickness, 6.9 for raster angle, 4.4 for part orientation			
	0.3	0/90	Vertical						
FDM		0		Immersion time of 180 s, 300 s, 420 s		25.63–34.7	1.88–7.64		Galantucci et al. (2010)
		30				28.45–37.32	3.03–6.63		
		60				41.52–52.94 for untreated	2.74–16.78 for treated		
FDM/AB[a]S	0.254	45°		Acetone vapour bath		0.82			Lalehpour and Barari (2016)
	0.33					1.34			
PJ	0.016	0	0–90	Finish type Matte, Glossy		1.5–15.1			Udroiu et al. (2019)
		45				1.8–10.5			
		90				0.9–13.4			
FDM		90				16.5–5.5			Boschetto and Bottini (2015)
		0				17–8.5			
		54				22-Dec			
		144				33.5–21.5			
FDM/ABS[a]	0.254					17 for initial	2.5 for finishing		Boschetto et al. (2016)
SL/TSR[b], Somos[c], Accura[d]			0			1	22	3	Kim and Oh (2008)
FDM/ABS[a]			30			18–21	49	6	
PJ/Epoxy resin			60			Aug-13	21	10	
			90			03-May for SL	18 for FDM	22 for PJ	
FDM	0.1778	0				9.5	13.27		Nan-charaiah et al. (2010)
	0.254	30				14.3	13.17		
	0.33	45				15.2 for layer thickness	13.08 for raster angle		
FDM		0		Vapour smoothing		3.01–3.9	0.22–0.9		Chohan et al. (2016)
		90				8.45–8.96 for initial	0.54–2.5 for final		

[a] ABS means acrylonitrile butadiene styrene

[b] TSR represents epoxy

[c] Somos represents resin for stereolithography

[d] Accura means ABS-like-material

Although it is not obvious that raster angle and part orientation affect the surface quality of FDM parts (Huang et al. 2019), a minimum number of layers should be selected during the setup of part orientation to consider the surface quality of wearables (Jin et al. 2016) due to the importance of build slopes of AM parts (Lalehpour & Barari 2016). The best surface roughness of PJ parts was at the 0° slope (Udroiu et al. 2019) but the best and worst for FDM parts were at the 90° slope and 0° slope, respectively (Boschetto & Bottini 2015). Additionally, the part orientation in both PJ and FDM affects the amount of support material, build time, etc. Particularly, PJ provides

an option of two finish types which affects the amount of support materials as well as surface quality (Udroiu et al. 2019, Table 2). Therefore, if users determine the best option based on an understanding of the condition which can increase material waste, it can help to reduce environmental impact.

Roughness is also increased by interaction with the support material and part material. It can make support removal hard and lead to additional expense and time (Lalehpour & Barari 2016). Therefore, a minimum support structure should be determined for the good surface quality of wearables (Jin et al. 2016) and a worksheet, which can screen the 3D CAD model, can be used to check whether surface finish is destructed, based on the existence or lack of support structure generation (Booth et al. 2017). These efforts can also reduce the lead time through depleting the time for the postprocess stage.

Furthermore, postprocess stage can be demanded for obtaining superb surface quality for AM parts (Lalehpour and Barari 2016). The types of postprocess are chemical, machining, and heat treatment (Garg et al. 2017). A research study used chemical treatment for FDM parts, and the surface finish is dramatically improved by chemical reaction which is controlled by soaking time of 300 s (Galantucci et al. 2009). In addition, the surface finish may be superior when chemical treatment is repeatedly conducted in the form of small durations of smoothing (30 s) (Garg et al. 2016). The effect of chemical treatment has no difference between a part built with thick layer thickness and one built with thin layer thickness but shows the various improvement of surface roughness depending on the part orientation (Lalehpour & Barari 2016). In addition, various machining treatments such as CNC and electropolishing are used to get rid of the rough surface of AM parts enhancing durability (Boschetto et al. 2016; Wan et al. 2019). Surface quality and porosity highly affect fatigue performance, and heat treatment can be essential to reduce residual stress, porosity and surface quality (Kim et al. 2018). Heat treatment has a positive effect on reflectivity, although a shrinkage effect of 10% appears. Different temperatures should be applied depending on the part materials (Chen et al. 2019). In addition, build slope affects the material removal rate and final part performance in post-treatment like barrel finishing (Boschetto & Bottini 2015). Therefore, effective setup of the AM process parameters and materials should be determined depending on the type of postprocess, because the effect of some parameters of AM processes can be offset by the type of postprocess. These users' behavior can reduce build time and resource waste which would minimize the environmental impact.

In addition, humidity and electrostatics affect the flow of powder and drying or monitoring powder may be demanded before building (Craik & Miller 1958). Electrostatic properties of particles can occur during sieving and handling powder and crystalline defects, impurities, moisture, and the stress on the powder due to milling and temperature are also influential factors (Yang & Evans 2007). Bad powder quality, humidity in materials and recycling powder can deteriorate surface quality (Bahr & Westkamper 2018; Moges et al. 2019). Therefore, creating the principle of material storage will help to establish the reliability of wearables fabrication.

Influence of AM process parameters on geometric properties

Part deformation, which can cause part failure, can require a postprocess stage and result in resource waste which increases environmental impact (Fig. 2). Especially, the deformation of FDM parts is affected by several factors; the setup of the process parameters, tool path generation, material characteristics, etc. (Wang et al. 2007). Part deformation is induced by residual stresses which can increase according to raster width although layer thickness affects them as well (Nancharaiah et al. 2010, Table 3). In addition, shell thickness affects both dimensional accuracy (Lanzotti et al. 2015) and successful fabrication of parts in the assembly (Booth et al. 2017). For instance, a flexible robotic hand which may apply to wearables can be designed, ensuring shell thickness of less than 10 mm to prevent deformation (Scharff et al. 2017).

Part orientation is also an influential parameter on residual stress and distortion (Mercelis & Kruth 2006). Inappropriate part dimensions induce the disuse of the fabricated part or the postprocess, and this is not an insignificant problem in terms of environmental impact. Part orientation in FDM affects dimensional accuracy, support structure, build time, the amount of material consumption, overhang, etc. (Jin et al. 2016). However, PJ, which shows a different tendency to other AM processes, promotes the accuracy of part's thickness and width on the z-axis (Barclift & Williams 2012) and dimensional accuracy differs depending on the part geometries and build slope which shows benefit on 45° slope (Khoshkhoo et al. 2018). Therefore, the prudent decision in part orientation should be made by users if they assign importance to dimensional accuracy. It is directly related to build time and resource consumption.

In addition, air gap highly affects dimensional accuracy rather than surface quality (Vasudevarao et al. 2000). An increment in the air gap results in not a change in the part length but the decrement of the part width (Guan et al. 2015). The nonuniform stress distribution is generated by the tool path, and residual stresses are high on the bottom of the FDM part (Mercelis & Kruth 2006). In addition, LS part shrinkage results from a part which is located far from the center because the bed temperature is nonuniform (Soe et al. 2013). Therefore, the air gap, tool path and part position may cause resources waste through the failure of AM wearable fabrication. Furthermore, Dimensional tolerance is affected by part geometry, part size and part thickness (Xu et al. 1999). Part size is largely related to the reduction of curling (Seo 2012) and a part with long height on the z-axis causes a large amount of deformation (Spisak et al. 2014). Tensile strength is induced by part orientation and the size of the surface area can cause distortion (Gibson & Shi 1997). However, part deformation and overhang were prevented by support structures in FDM wearables (Jin et al. 2016).

However, temperature profile plays an essential role in part performance. Shrinkage behavior in FDM is determined by glass transition temperature (T_g), and shrinkage rate can be linearly formulated for the material with low T_g and short fibre length (Es-Said et al. 2000). For instance, PLA is advantageous for low warping and low environmental impact (Bahr & Westkamper 2018). The characteristics of PLA promote deformation and yield strength, and a sample of PLA shows less deformation and higher yield strength than that of ABS (Ebel & Sinnemann 2014). Cooling of material from T_g to envelope temperature causes inner stresses and deformation such as cracking or fabrication failure, and the desirable envelope temperature is 70 °C for ABS (Wang et al. 2007).

Table 3 Influential AM parameters on dimensional accuracy

AM process	Layer thickness (mm)	Air gap (mm)	Raster angle	Part orientation	Outcome			Ref.
					Warp deformation or dimensional accuracy (mm)/shrinkage (%)			
SL FDM LS			0		Part A	Part B		Kim and Oh (2008)
			30		94% for 0.2	85% for 0.2		
			60		84% for 0.15	72% for 0.15		
			90		70% for 0.1	55% for 0.1		
					42% for 0.05 in SL	28% for 0.05 in SL		
					88% for 0.2	90% for 0.2		
					73% for 0.15	80% for 0.15		
					61% for 0.1	61% for 0.1		
					4% for 0.05 in FDM	40% for 0.05 in FDM		
					78–88% for 0.2	97–99% for 0.2		
					71–77% for 0.15	92–97% for 0.15		
					58–61% for 0.1	78–92% for 0.1		
					34–39% for 0.05 in LS	52–70% for 0.05 in LS		
FDM			Raster, contour, contour/raster		0.1–1.8			Wang et al. (2007)
FDM	0.1778	−0.001	0		25.63	25.68	25.68	Nancharaiah et al. (2010)
	0.254	0	30		25.64	25.67	25.6	
	0.33	+0.001	45		25.7 for layer thickness	25.65 for raster angle	25.67 for air gap	
		0.001						
		0.002						
LS	Laser power (W) 24, 28, 32, 36	Scan speed (mm/s) 3000, 3500, 4000, 4500	Part bed temperature © 175, 176, 177, 178	X	0.37–1.13			Raghunath and Pandey (2007)
		Hatch spacing (mm) 0.22, 0.24, 0.26, 0.28	Scan length (mm) 30, 45, 60, 75	Y	0.38–1.32			
				Z	2.65–4.02			

Table 3 (continued)

AM process	Layer thickness (mm)	Air gap (mm)	Raster angle	Part orientation	Outcome	Ref.
					Warp deformation or dimensional accuracy (mm)/shrinkage (%)	
SL				Three types of orientation	Volume of inaccuracy	Xu et al. (1999)
LS					3.75 (SL), 3.75 (LS), 3.35 (FDM) for orientation 1	
FDM					3.35 (SL), 3.35 (LS), 2.31 (FDM) for orientation 2	
					3.36(SL), 3.36(LS), 2.31(FDM) for orientation 3	

Therefore, heating the chamber can be a technique to ensure uniform cooling which results in the reduction of thermal distortion (Stansbury & Idacavage 2016). In addition, the increase in temperature on tank surface is based on energy input in SL, and low scan speed can cause shrinkage and curling, which are induced by high temperature and reaction rates (Corcione et al. 2006). Part distortion in LS also results from huge thermal differentials in the build bed (Stansbury & Idacavage 2016). Remaining the sintered material between melting and recrystallizing temperatures can cause low part distortion and reduce the accumulation of residual stresses (Fulcher & Leigh 2012). Furthermore, the shrinkage rate, which is caused by the amount of crystallinity, can decrease as energy density increases (Raghunath & Pandey 2007). Therefore, maintaining uniform envelope temperature is essential to fabricating wearables with low deformation, so that the role of the user in monitoring the envelope temperature during printing becomes more important. However, nonlinear shrinkage occurs if polymeric material rapidly cools. The problem can be also solved by conducting a postprocess stage (Vasudevarao et al. 2000). Sintering treatment is utilized to improve the accuracy for a part with ceramics (Ebert et al. 2009) but a part with hydroxyapatite can also undergo shrinkage (Fierz et al. 2008). Heat treatment results in excellent reflectance and a considerable deformation (Chen et al. 2019) and chemical treatment causes a reduction of dimensional change (Chohan et al. 2016). Therefore, it may be necessary to determine the proper condition of postprocess by the parameters of AM processes.

Influence of AM process parameters on mechanical properties

The evaluation of the mechanical properties of AM wearables is about stiffness, compressive behavior, impact energy and so on (Table 1). However, it is hard to define the minimum part properties because mechanical properties are influenced by various parameters of the AM preprocess, inprocess, and postprocess stages (AMSC 2017). In other words, user behavior, which determines the parameters of AM processes, affects the part properties (Fig. 2). Therefore, this section identifies the parameters of the AM process that affect mechanical properties covered by AM wearables studies: tensile, and flexural properties, elastic performance, compressive properties, etc.

Anisotropy formed by printing direction is a characteristic of performance (Es-Said et al. 2000, Table 4) and part orientation is an essential parameter in AM (Raut et al. 2014b). The influences of part orientation on tensile strength vary in AM processes and FDM shows that tensile strength is the highest on the y-axis (Fig. 3). Flexural strength is

Table 4 Influential FDM process parameters on tensile properties and hardness

AM process /material	Layer thickness (mm)	Number of shell	Air gap	Part orientation	Raster angle	Postprocess stage	Material quality	Tensile strength (MPa)	Tensile stress (MPa)	Ref.
FDM/ABS[a]	0.1			Horizontal	45/− 45		Filament dried in vacuo for 4 h at 80 °C	12–33.6		Huang et al. (2019)
	0.2			Lateral	30/− 60			Difference between max and min		
	0.3			Vertical	0/90			9.3 for layer thickness		
								1.1 for raster angle		
								11.1 for part orientation		
FDM					0	Immersion time of 180 s, 300 s, 420 s		18.1–19.8 16.3–18.43		Galantucci et al. (2010)
					30			19.24–20.77 16.21–20.09		
					60			19.63–21.21 for untreated 15.23–17.85 for treated		
FDM/PLA	0.1			Xyz	90/180			4.9–21.5		Torres et al. (2016)
	0.3			Xzy	45/135			2.3–15.5		
				Yzx				May-36		
								2.3–36 for 90/180		
								2.4–27.5 for 45/135		
FDM				X	0			30.28–33 19–35.45		Raut et al. (2014a)
				Y	45			28.52–35.45 22.51–30.28		
				X	90			17.14–22.51 for part orientation 17.14–34.31 for raster angle		
FDM/ABS[a]					45/− 45			13.7		Es-Said et al. (2000)
					0			20.6		
					45			7		
					90			9.3		
					45/0			14		

Table 4 (continued)

AM process /material	Layer thickness (mm)	Number of shell	Air gap	Part orientation	Raster angle	Postprocess stage	Material quality	Tensile strength (MPa)	Tensile stress (MPa)	Ref.
FDM/ABS[a]					0				30.96	Huang and Singamneni (2015)
					15				29.35	
					30				25.83	
					45				18.33	
					60				13.52	
					75				11.64	
					90				10.08	
FDM/PLA					0				68.1	Zhang et al. (2019)
					90				52.85	
					45				67.12	
					0/90				57.89	
					− 1				62.11	
FDM/PLA					X				38.7	Afrose et al. 2016)
					Y				31.1	
					45				33.6	
FDM/ABS[a]			− 0.05		0/90			33.1		Dawoud et al. (2016)
			0.05		30/− 60			33.2		
					45/− 45			34.3		
					75/− 15			33.4		
					0/90			28.1		
					30/− 60			30.4		
					45/− 45			31.7		
					75/− 15			30.4		

Table 4 (continued)

AM process /material	Layer thickness (mm)	Number of shell	Air gap	Part orientation	Raster angle	Postprocess stage	Material quality	Tensile strength (MPa)		Tensile stress (MPa)	Ref.
FDM/PC[b]	5				0			19.03			Hill and Haghi (2014)
					15			18			
					30			24.3			
					45			24.13			
					60			38.89			
					75			44.75			
					90			59.78			
FDM/PLA	0.05		0		45/− 45			9.62–30.77	11.15–30.77		Li et al. (2017)
	0.15		0.2					6.74–24.62	8.08–18.27		
	0.25		0.4					5.96–15.38 for layer thickness	5.96–12.5 for air gap		
FDM					Vertical, horizon			31.2–38.9			Yang et al. (2015)
								29.7–37.1			
FDM/ABS[a]			0.127, 0.254, 0.381	ZXY				15–41			Spisak et al. (2014)
				XYZ				18–73			
				XZY				42–86			
FDM/ABS[a]				Longitudinal, transverse	0, 90, 45, −45			17.9–31.2, 13.4–13.6			Rodriguez et al. (2000)
SL/TSR[c], Somos[d], Accura[e]	0.15/0.1/0.1			Horizontal, vertical				42–56	49–71		Kim and Oh (2008)
FDM/ABS[a]	0.254							17–50	Nov-25		
LS/PA[f]	0.1/0.15							29–49	26–39		
PJ/Epoxy resin	0.016							62 for horizontal	29 for vertical		

Table 4 (continued)

AM process /material	Layer thickness (mm)	Number of shell	Air gap	Part orientation	Raster angle	Postprocess stage	Material quality	Tensile strength (MPa)			Tensile stress (MPa)	Ref.
FDM/ABS[a]				YZX	0	Chemical untreatment/ chemical treatment and along the length/ across the length		31–34	23–33			Garg et al. (2017)
				YXZ	30			32.5–33	24–31			
				ZYX	60			15–28 for untreatment	18–32 for treatment			
					90							
FDM/PLA	0.1	2			0			49.29	42.28	53.59		Lanzotti et al. (2015)
	0.12	3			18			45.58	44.82	50.51		
	0.15	4			45			48.01	48.49	48.09		
	0.18	5			72			48.95	49.71	44.02		
	0.2	6			90 (reduction of strength and stiffness			48.49 for layer thickness	50.67 for the number of shells	43.39 for infill orientation		

[a] ABS means acrylonitrile butadiene styrene

[b] PC means polycarbonates

[c] TSR represents epoxy

[d] Somos represents resin for stereolithography

[e] Accura means ABS-like-material

[f] PA means polyamide

the highest on the x-axis (Raut et al. 2014a) and the lowest on the z-axis (Jin et al. 2016). Many studies have shown the highest tensile strength in build orientation of xzy and the difference in strength has shown to be more than 40% between build orientations. On the other hand, Das et al. (2018) shows that tensile strength in PJ is the highest at the build orientation of xyz with raster angle of 0° and the lowest at build orientation of xzy with raster angle of 90° (Table 5), and elongation at break in build orientation of xzy with raster angle of 0° is the highest. However, tensile strength in LS is irregularly influenced by part orientation. Tensile strength is the highest at yzx (Gibson & Shi 1997, Table 6) and increases by 790% at horizontal orientation (Eshraghi & Das 2010) but part orientation does not affect tensile strength (Majewski & Hopkinson 2011). Taken together, previous studies have shown that the effect of part orientation on tensile strength is inconsistent. Different AM processes seem to have different effects of part orientation, and comprehensive experimental design would be required.

Part orientation has various influences on compressive strength, depending on AM processes. FDM parts with a cylinder shape have four times higher compressive strength than parts built using the inkjet process with a binder. Compressive strength is the highest for an FDM part built perpendicularly from load direction but the lowest for an inkjet part (Lee et al. 2007). There is a fourfold difference between the two AM processes. Compressive strength is higher for an SL part built perpendicularly in the force direction (297 MPa) than for a part built in the horizontal direction (257 MPa) (Alharbi et al. 2016). These outcomes show that users should determine part orientation after considering the load direction of the AM part. Therefore, users should understand not only the parameter characteristics of AM processes, but also the characteristics of wearables based on their intended use, in order to fabricate AM parts with high performance.

In general, mechanical properties decrease as raster angle increases. 0° raster angle shows the highest ultimate tensile stress, elastic modulus, tensile strength, and flexural strength (Huang & Singamneni 2015; Zhang et al. 2019; Table 7). Raster angle determines bonding on cross-sections formed on an FDM part (Sun et al. 2008). In addition, tensile strength is the highest at a 45/−45° part compared with a 0/90° part. However, flexural strength is the highest for a 0/90° part (Dawoud et al. 2016, Table 8). Hardness is the highest for each 0° and 90° part (Hill & Haghi 2014). Raster angle affects mechanical properties but bond strength between filaments affects the properties rather than the raster angle itself. Mechanical properties such as hardness can be considered essential for wearables because elastic and plastic changes in the shape from external stimuli should critically affect the functionality and durability of the AM part.

In addition, air gap, layer thickness and tool path generation affect porosity. A negative gap maximizes the bond strength and minimizes porosity (Rodriguez et al. 2000). Different raster angles are required to achieve superior mechanical properties, and a specific raster angle should be determined to ensure a particular mechanical property. Raster angle and air gap play a critical role in determining mechanical properties of an FDM part and the properties of the FDM part can be comparable to those of parts fabricated by injection molding (Dawoud et al. 2016). Particularly, they are crucial to tensile and compressive properties (Li et al. 2017) and the increase in the air gap decreases flexural strength (Guan et al. 2015). Smaller layer thickness also affects lower porosity (Huang et al. 2019) and higher bond strength (Amorim et al. 2014)

Table 5 Influential SL and material jetting process parameters on tensile properties and hardness

AM process / material	Layer thickness (mm)	Part orientation	Other parameters	Postprocess stage	Tensile strength (MPa)		Young's modulus, E (MPa)		Hardness	Ref.
PJ/ROM[a]		Flat-X			58.58					Das et al. (2018)
		Flat-45			57.62					
		Flat-Y			53.82					
		Vert-X			54.26					
		Vert-45			56.32					
		Vert-Y			53.4					
SL/TSR[b], Somos[c], Accura[d]	0.15/0.1/0.1	Horizontal, vertical			42–56	49–71			97	Kim and Oh (2008)
FDM/ABS[e]	0.254				17–50	Nov-25				
LS/PA[f]	0.1/0.15				29–49	26–39				
PJ/Epoxy resin	0.016				62 for horizontal	29 for vertical				
PJ/ABP[g]		ZX			58.28				80.23	Kesy and Kotlinski (2010)
		XZ			60.44				77.78	
		XY			41.65				77.18 for Shore	
PJ/ROM[a], ABP[g]				Room T, liquid nitrogen T, immersed in liquid helium	32–36		2497–8876			Weiss et al. (2015)
FDM/ABS					32–43		2583–5570			
PJ/ROM[a]	3.22–3.66	XYZ	Part spacing: tight vs. far		35.3	29	1665	1719		Barclift and Williams (2012)
		YXZ			32.3	26	1501	1577		
		YZX			31.2	24.2	1696	1176		
		XZY			37.8 for tight	22.9 for far	1874 for tight	1284 for far		

[a] ROM means a rigid opaque material called VeroWhite

[b] TSR represents epoxy

[c] Somos represents resin for stereolithography

[d] Accura means ABS-like-material

[e] ABS means acrylonitrile butadiene styrene

[f] PA means polyamide

[g] ABP means acrylic-based-photopolymer called Fullcure

Table 6 Influential LS process parameters on tensile properties and hardness

AM process / material	Layer thickness (mm)	Part orientation	Raster angle	Other parameters	Postprocess stage	Material quality	Tensile strength (MPa)		Young's modulus, E (MPa)	Hardness	Ref.
LS/semi-crystalline polymers		VV	PV (90)	Part bed temperature (3–4 °C below melting T)	Coating, surfaces finishing		17	35		66–70 for no coating, 75 for coating	Gibson and Shi (1997)
		VP	PP (0)	Fill laser power			15	40			
		VZ		Scan size (55–85)			5 for part orientation	40			
				Scan spacing (0.11–0.17), building height level (1–5)			Fill laser power (13–35), scan size (12–24)	37			
							Scan spacing (10–27), no orientations (6–17), no coating (34–39), coating (36–41)	33 for building height level from layer 1 to layer 5			
LS/polycaprolactone		Parallel					10.5		363.4		Eshraghi and Das (2010)
		Perpendicular					16.1		343.9		
LS/Nylon12	02-Jun	YX					50		2260		Majewski and Hopkinson (2011)
		YZ					47		2500		
		ZY					49		2000		
LS/Nylon12						L_Virgin	35		1620		Zarringhalam et al. (2006)
						L_Refresher	33		1400		
						L_Used	42		1625		
						T_Virgin	46		1760		
						T_Refresher	48		1760		

Table 6 (continued)

AM process / material	Layer thickness (mm)	Part orientation	Raster angle	Other parameters	Postprocess stage	Material quality	Tensile strength (MPa)		Young's modulus, E (MPa)	Hardness	Ref.
SL/TSR Somos Accura	0.15/0.1/0.1	Horizontal, vertical					42–56	49–71		Rockwell	Kim and Oh (2008)
FDM/ABS	0.254						17–50	Nov-25		97	
LS/PA[a]	0.1/0.15						29–49	26–39		68–105	
PJ/Epoxy resin	0.016						62 for horizontal	29 for vertical		87–93	
LS/HIPS					Infiltrating		4.59 (7.54 after infiltrating)		–		Yan et al. (2010)
HIPS.epoxy							18.63		–		
PA12							38.3		1420		
PA12.OREC[b]							50.9		–		
Nanosilica/PA12							46.3		1980		

[a] PA means polyamide

[b] OREC means organically modified rectorite

Table 7 Influential FDM process parameters on Young's modulus and hardness

AM process / material	Layer thickness (mm)	Number of shell	Part orientation	Raster angle	Postprocess stage	Young's modulus, E (MPa)	Hardness	Ref.
FDM/PLA[a]	0.1		XYZ	90/180		490–2200		Torres et al. (2016)
	0.3		XZY	45/135		500–2400		
			YZX			650–3100		
						500–2400 for 90/180		
						490–2200 for 45/135		
FDM/PLA[a]				0		5260		Zhang et al. (2019)
				90		4780		
				45		5080		
				0/90		4860		
				+45/-45		4980		
FDM/PLA[a]				X		1538		Afrose et al. 2016)
				Y		1246		
				45		1350		
FDM/PC[b]	5			0		1420.3	104.6	Hill and Haghi (2014)
				15		1351.37	89.4	
				30		1461.69	93	
				45		1358.27	91.8	
				60		1744.37	95.4	
				75		1958.11	103.7	
				90		2082.22	103.8 for Rockwell	
FDM				Vertical, horizon		8.5–10.4		Yang et al. (2015)
						8.1–9.9		
FDM/ABS[c]			Longitudinal, transverse	0, 90, 45, − 45		1400–1986		Rodriguez et al. (2000)
SL	0.15/0.1/0.1		Horizontal, vertical				97	Kim and Oh (2008)
FDM/ABSc	0.254						68–105	
LS	0.1/0.15						87–93	
PJ	0.016						–	

Table 7 (continued)

AM process / material	Layer thickness (mm)	Number of shell	Part orientation	Raster angle	Postprocess stage	Young's modulus, E (MPa)			Hardness		Ref.
FDM/PLA[a]	0.1	2		0		3497.63	2951.83	3388.57			Lanzotti et al. (2015)
	0.12	3		18		2962.15	3002.23	3227.89			
	0.15	4		45		3030.56	3125.03	3087.2			
	0.18	5		72		3229.09	3189.01	2963.35			
	0.2	6		90		3256.77 for layer thickness	2857.8 for number of shells	2799.43 for infill orientation			
FDM/ABS[c] PLA[a]				Honeycomb, line pattern		900–950 1200–1450 for honeycomb	1300–1900 1900–2600 for line pattern				Ebel and Sinnemann (2014)
FDM/ABS[c]			X Y Z	0 90	Vapour smoothing				70.5–83 46.5–60.5 for initial	76–90 50–66 for final	Chohan et al. (2016)

[a] PLA means polylactic acid

[b] PC means polycarbonates

[c] ABS means acrylonitrile butadiene styrene

Table 8 Influential FDM process parameters on flexural, and impact strengths

AM process / material	Layer thickness (mm)	Number of shell	Air gap (mm)	Part orientation	Raster angle (°)	Postprocess stage	Material quality	Flexural strength (MPa)		Impact strength (KJ/m^2)	Ref.
FDM/ABS[a]	0.1			Horizontal	45/−45		Filament dried in vacuo for 4 h at 80 °C	27.3–64.4		4.64–21.51	Huang et al. (2019)
	0.2			Lateral	30/−60			Difference between max and min		Difference between max and min	
	0.3			Vertical	0/90			9.3 for layer thickness		2.39 for layer thickness	
								6.1 for raster angle		2.4 for raster angle	
								30.8 for part orientation		13.99 for part orientation	
FDM					0	Immersion time of 180 s, 300 s, 420 s		38.63–40.65	40.51–46.63		Galantucci et al. (2010)
					30			40.30–42.99	40.88–45.18		
					60			41.53–44.35 for untreated	40.26–45.31 for treated		
FDM				X	0			30.67–45.20	28.2–45.2		Raut et al. (2014a)
				Y	45			28.01–39.61	27.44–38.62		
				X	90			27.44–36.41 for part orientation	30.67–39.61 for raster angle		
FDM/ABS[a]					45/−45			33.1		0.77 J	Es-Said et al. (2000)
					0			44.4		4.12 J	
					45			31.1		0.78 J	
					90			19.6		0.36 J	
					45/0			32.2		0.93 J	

Table 8 (continued)

AM process / material	Layer thickness (mm)	Number of shell	Air gap (mm)	Part orientation	Raster angle (°)	Postprocess stage	Material quality	Flexural strength (MPa)		Impact strength (KJ/m^2)	Ref.
FDM/ABS[a]			−0.05		0/90			64		40	Dawoud et al. (2016)
					30/−60			60.7		35.9	
					45/−45			62.2		41.9	
					75/−15			61.9		33.9	
			0.05		0/90			42		26.2	
					30/−60			44.2		32.2	
					45/−45			49.8		38	
					75/−15			32		18.2	
FDM			0.5					235			Guan et al. (2015)
			0.7					190			
			0.9					150			
			1.1					130 N			
FDM/ABS[a]				YZX	0	Chemical untreatment/ chemical treatment		49–58	48–54		Garg et al. (2017)
				YXZ	30			49–54	40–44		
				ZYZ	60			23–39 for untreatment	18–32 for treatment		
					90						

[a] ABS means acrylonitrile butadiene styrene

Table 9 Influential FDM process parameters on compressive and yield strengths and elongation at break

AM process / material	Layer thickness (mm)	Number of shell	Part orientation	Raster angle (°)	Compressive strength (MPa)	Yield strength (MPa)	Elongation (%)	Ref.
FDM/ PLA[a]	0.1 0.3		XYZ XZY YZX	90/180 45/135		Apr-20 2.3–14 4.8–32.5 2.3–32 for 90/180 2.24–25.5 for 45/135		Torres et al. (2016)
FDM/ ABS[b]				45/− 45 0 45 90 45/0		10.4 16.3 6.6 7.9 13.6		Es-Said et al. (2000)
FDM			Horizontal, vertical, diagonal	45/− 45	41.3 37			Lee et al. (2007)
FDM/ PLA[a]				0 90 45 0/90 − 1			6.52 5.58 6.31 5.89 6.04	Zhang et al. (2019)
FDM/PC[c]	4.97–5	0.197		0 15 30 45 60 75 90		18.62 16.89 19.51 17.79 27.3 34.47 40.2	1.57 1.64 2.14 2.64 3.17 2.81 3.89	Hill and Haghi (2014)
FDM/ ABS[b]			Longitudinal, transverse	0, 90, 45, − 45		24.4–17.9 13.6–13.4		Rodriguez et al. (2000)
FDM/ ABS[b] PLA[a]				Honeycomb, line pattern		14.5 18–22 for honeycomb	20–32.5 42 for line pattern	Ebel and Sinnemann (2014)

[a] PLA means polylactic acid

[b] ABS means acrylonitrile butadiene styrene

[c] PC means polycarbonates

of AM parts which are related to mechanical properties. The effect of layer thickness on mechanical properties is the most important variable in the inkjet process with a binder which can affect part strength (Galantucci et al. 2010), but the effect is irregular in FDM (Luzanin et al. 2017). For example, Torres et al. (2016) found that layer thickness did not necessarily have an effect on strength (Table 9) and Galantucci et al. (2010) found that layer thickness influenced mechanical properties along with other parameters. Therefore, shell thickness may be a more important variable on ultimate tensile strength than layer thickness (Lanzotti et al. 2015) although layer and shell thicknesses can be affected by various factors such as materials, 3D geometries, etc. Furthermore, tool path generation affects porosity (Kim et al. 2018) and the cooling rate which influences bond strength between neighboring filaments (Sun

et al. 2008). Porosity has an injurious effect on the tensile and flexural strengths of a part fabricated by filaments (Barbero 2011). The tool path which consists of a number of short lines can negatively affect the build time and infill quality of wearables, and a wavy path imposes a better change on flexural strength than a zigzag path (Jin et al. 2016). In addition, the tensile strength of a part with a solid infill can only increase the tensile strength by 20% while an infill percentage of 10% (Yang et al. 2015) and contours on the outside can reduce material consumption (Spisak et al. 2014). These studies indicate that material savings can be achieved through determination of the optimized infill percentage.

Part spacing affects tensile strength and tight part spacing affects high tensile strength and modulus on yzx or xzy orientation. UV exposure time can affect the mechanical properties of PJ parts, and the parts, which are close to other parts, can be overcured by UV light (Kim & Oh 2008). In addition, the edge of PJ part, which is located in parallel at a jetting direction, has higher density and is harder than the center of the part (Kesy & Kotlinski 2010). Meanwhile, a LS part, which is in the middle of the chamber, presents higher tensile strength and part density because high temperatures can be maintained during sintering (Gibson & Shi 1997).

Moreover, postprocess can lead to enhanced mechanical properties as well as surface topography (Kim et al. 2018). Acetone has advantages for the chemical treatment of ABS parts because it has low toxicity, low cost expense and a high rate of evaporation (Garg et al. 2017), and vapor smoothing with solvent can be used for some polymers (AMSC 2017). The chemical treatment is dependent on the material chemistry, and the secondary bonds are weakened on the surface which comes into contact with the acetone vapors. The layers can reach a stable position through filling the pores between layers, and the reaction solidifies the surface in the form of a smooth texture (Garg et al. 2017). The improvement of surface topography through acetone increases compressive and flexural strength (Kuo & Mao 2016) although tensile strength decreases (Percoco et al. 2012). In addition, heat treatment imposes various effects on mechanical properties depending on part orientation (Cox et al. 2015). For instance, a part fabricated on a y-axis had higher compressive strength in the application of furnace and vacuum oven temperatures of 60 °C. Drying time also affects strength. Thus, the type and operating conditions of the postprocess determined by users impose an impact on mechanical properties.

Material selection also affects mechanical properties of AM parts, and the mechanical properties of an FDM part for ABS and a PJ part for a rigid opaque material (ROM) called VeroWhite which is manufactured from a mixture of different photopolymer materials differ. Tensile properties were similar between the two parts, but the PJ part exhibits higher compressive modulus, and ultimate strength than the FDM part (Weiss et al. 2015, Table 10). Mechanical properties increase for LS parts fabricated with composites when high impact polystyrene (HIPS) with epoxy (four times in tensile strength) and Polyamide12 (PA12) with nanosilica (25% for tensile strength) are compared with HIPS and PA12, respectively (Yan et al. 2010). Fresh, virgin and used powder, which all have different molecular weight, also promote diverse ductility and elongation at break for LS parts (Zarringhalam et al. 2006, Table 11). In addition, the humidity of materials significantly affects mechanical properties (Bahr & Westkamper 2018). Therefore, it can

Table 10 Influential SL and material jetting process parameters on other mechanical properties

AM process / material	Layer thickness (mm)	Part orientation	Postprocess stage	Impact strength (KJ/m^2)		Compressive strength (MPa)		Yield strength (MPa)	Elongation (%)	Ref.
PJ/ROM[a]		Flat-X							6.57	Das et al. (2018)
		Flat-45							6.45	
		Flat-Y							6.21	
		Vert-X							7.28	
		Vert-45							6.94	
		Vert-Y							6.51	
SLA/composite resin		Horizontal, vertical				257.7 297.7				Alharbi et al. (2016)
SL/TSR[b], Somos[c], Accura[d]	0.15/0.1/0.1	Horizontal, vertical		Peak load (N) 450	Peak load (N) 390	54	50			Kim and Oh (2008)
FDM/ABS[e]	0.254			470–820	160–440	41–65	42–66			
LS/PA[f]	0.1/0.15			390–690 for horizontal	490–770 for vertical	60–72 for horizontal	61–73 for vertical			
PJ/ABP[g]		ZX							9.26	Kesy and Kotlinski (2010)
		XZ							23.44	
		XY							4.04	
PJ/ROM[a], ABP[g]			Room T, liquid nitrogen T, immersed in liquid helium			86–431		32		Weiss et al. (2015)
FDM/ABS[e]						50–101		33		

[a] ROM means a rigid opaque material called VeroWhite

[b] TSR represents epoxy

[c] Somos represents resin for stereolithography

[d] Accura means ABS-like-material

[e] ABS means acrylonitrile butadiene styrene

[f] PA means polyamide

[g] ABP means acrylic-based-photopolymer called Fullcure

Table 11 Influential LS process parameters on other mechanical properties

AM process / material	Layer thickness (mm)	Part orientation	Postprocess stage	Material quality	Flexural strength (MPa)	Impact strength (KJ/m^2)	Compressive strength (MPa)	Yield strength (MPa)	Elongation (%)	Ref.
LS/polycaprolactone		Parallel					38.7	12.5		Eshraghi and Das (2010)
		Perpendicular					38.8	10.3		
LS/Nylon12	02-Jun	YX							17.5	Majewski and Hopkinson (2011)
		YZ							17	
		ZY							11	
LS/Nylon12				L_Virgin					4	Zarringhalam et al. (2006)
				L_Refresher					7.5	
				L_Used					12.5	
				T_Virgin					14	
				T_Refresher					19	
LS/HIPS			Infiltrating		18.93 (20.48 after infiltrating)	3.3 (6.5 after infiltrating)			5.79 (5.98 after infiltrating)	Yan et al. (2010)
HIPS.epoxy					30.69	3.9			6.44	
PA12					50.3	30.4			20.83	
PA12.OREC[a]					67.3	33.8			18.2	
Nanosilica/PA12					–	40.2			20.07	

[a] OREC means organically modified rectorite

be seen that the user's selection of a material is important. The next section discusses the wearables studies about AM fabrication cases with AM process parameters.

AM wearables fabrication cases considering AM process parameters

This section discusses cases of AM wearables, such as examples of ankle foot orthoses (AFO) configuration to consider when determining the parameters of AM processes. Part size, material characteristics, AM process manufacturer, etc. induce differences in part finish, materials used, and the fabrication cost of AFO (Miclaus et al. 2017). Optimal function of AFOs requires personalized-fit (Croccolo et al. 2013), namely creating contoured surfaces at the foot and heel (Pallari et al. 2010). In particular, the wearer's motion can create stability in expansion and contraction if elastomer is applied to the particular regions of the product (Lunsford et al. 2016). In addition, AFO functionality such as the stiffness of rotation or bending can be fine tuned as optimized parameters of 3D CAD model generation which consists of optimal shape, size and thickness (Croccolo et al. 2013).

Figure 4a shows how AM process and material are selected for fabricating a durable AFO (Walbran et al. 2016). Human behaviors are involved in scanning lower limbs, filling voids, applying a smoothing filter, and using CREO software. However, in particular, Fig. 4a presents the procedure of determining AM process and material suitable for AFOs by conducting a combination of several AM process parameters to minimize the impact of human behavior. Figure 4b presents the AM fabricated conditions of AFOs on examining the effect of different levels of stiffness, and AFOs have the advantage of improving the functionality of gait and muscle with ease (Choi et al. 2017). Suitable shore hardness in the form of flexible hinges and soft edges enhance functionality and comfort (Davia-Aracil et al. 2018). Meanwhile, the damping characteristic, which is related to energy losses, can be altered by the part orientation of LS (Faustini et al. 2008), and multi-component AFOs may be the ideal choices because single-component AFOs cannot achieve maximum strength in all areas (Walbran et al. 2016; Wojciechowski et al. 2019). In addition, anisotropic strength through a parallel tool path might cause poor mechanical properties for AM AFOs (Jin et al. 2016) although AM fabrication would be advantageous in terms of lead time and material costs (Pallari et al. 2010). Therefore, the appropriate parameters for AM processes should be determined in order to fabricate a successful final part.

Meanwhile, many wearables studies focus on materials and the design for obtaining the functionality of wearables depending the usage purpose, and AM processes themselves have a low profile in AM wearables. The characteristics of shape-memory materials (SMM) apply to wearables such as prosthesis through using leaf springs. Heat stimuli is used in electronics and camouflage technology, which makes color and structure changed, is used in textiles. It helps ventilation system and insulation on garments (Ali et al. 2019). Furthermore, SMM can be used for complex devices such as energy absorbers and soft robotic actuators, and Ituarte et al. (2019) studies a design and the workflow of manufacturing when using SMM. The study considers just part orientations of xyz, yxz and zyx as the AM process parameter and presents that elongation at break is highly

a

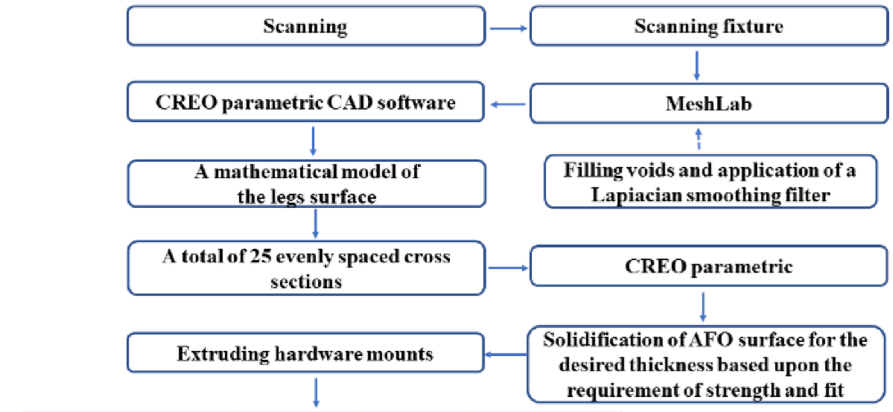

AM process type and material	LS with nylon	FDM with PLA	FDM high-modulus carbon fibre filled PETG
Yield stress (MPa)	-	88	97
Fracture stress (MPa)	28	-	-
Yield and fracture strain	-	Much higher	-

→ FDM with PLA

b

Condition of AM orthoses experiments	
3D CAD design	Scanning human body, Using mesh design software
AM process	Fused deposition modeling (FDM)
Filament	Polylactide (PLA)
Infill %	100%
Layer thickness (mm)	0.2
Number of shells	2
Stiffness (Nm/°)	0.25, 1, 2, and 3.7
Kinematics changes (Nm)	3.3, 11.6, 20.3, and 31.4

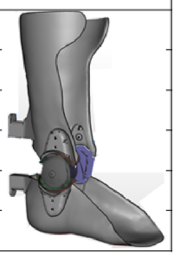

Fig. 4 Examples of AM AFO fabrication condition. *PETG means polyethylene terephthalate glycol

influenced by part orientation compared with ultimate tensile strength and Young's modulus.

Comotti et al. (2017) tries to improve functional design through the optimization of infill ratio and patterns and raster angle and suggests the necessity to customize the characteristics of infill depending on the requirement such as loads. The influence of raster angle is investigated when textiles are fabricated (Kozior et al. 2018). To reduce deformation of textiles, raster angle and adhesion force are considered. Adhesion force which may be related to tool path strategy are important although the effect of raster angle is not statistically significant. In addition, Santos et al. (2017) manipulates layer thickness, infill percent, orientation in the chamber and support material for producing four types of orthosis design, and the possibility is suggested for fabrication of orthosis based on customer needs.

Most studies mentioned above deal with limited AM process parameters. However, wearables design and fabrication must meet usage requirements, such as size or

Part orientation		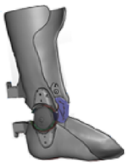	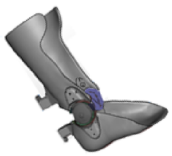
Surface quality	Worst	Best	In between
Layer number	Least	Most	In between
Support structure	Most	Least	In between
Bending strength	Best	Worst	In between

Fig. 5 Impact of part orientation in AM AFO. *Part orientation in the previous study was presented via the 3D CAD model of NIH AFO

weight limitations, geometrical characteristics, functionality (Kwon et al. 2017), contact with human skin, elasticity taking into account the part of the body to which it is to be applied, and pressure distribution, etc. (Davia-Aracil et al. 2018). So, it is necessary to consider these usage situations to determine the optimal AM process, part orientation and number of parts (Fig. 5) (Jin et al. 2016). In other words, it is necessary to fabricate a multi-piece product based on the functionality of the product, or to select a specific AM process (Walbran et al. 2016).

Requisites for desired performance in AM wearables

The attributes of the AM process itself make the users contemplate to achieve desired performance. It is hard to determine the minimum properties of AM wearables because various parameters of AM processes affect performance of wearables. In the current situation of worksite, the role of designers, who need to assess functional features through design revisions, are essential to enhance durability of AM parts (Liu et al. 2019).

Database construction considering the particular wearables application

Most wearables, fabricated by AM, would have complex geometries, and it is not easy to setup automatic part orientation to provide good performance for every different geometry. The human–machine interface would be helpful for users who do not have much knowledge of AM (Kuo & Su 2013), but it does not reflect the feature-based-approach required by AM (Zhang et al. 2016). Therefore, application-specific guideline to minimize the trial-and-error process undertaken by users may be required to fabricate wearables with good performance and to minimize the environmental impact through checking building feasibility and considering fabrication constraints (Fig. 2). Figure 2 presents each stage affected by performance, environmental impact and user behavior in AM wearables fabrication and provides decision stages to achieve 'building' without failure. To minimize the influence of user behavior on performance and environmental impact, the database construction in each AM process is required based on empirical research. Besides, when setting up various parameters, it is necessary to define the AM fabrication constraints that can be supplemented by understanding physical phenomena

involved in AM process. Since the settings of the parameters affect performance of wearables, developing AM fabrication constraints models through theoretical methods and applying them to the reliable human–machine interfaces can be an alternative.

Evaluation methods for AM wearables performance

Most of all, the first goal of reducing the environmental impact is to fabricate parts with desired performance without any failures. In other words, to enable the prediction of a part's lifetime may serve as a fundamental solution to minimize material waste and build time (Faludi et al. 2015; Rebaioli & Fassi 2017). It may be helpful to carefully follow the procedure in Fig. 2 when fabricating AM parts. There are two stages before building and it can be seen that user behavior is inevitably involved in the preprocess, inprocess and postprocess stages. Due to the attributes of AM processes, the setting of process parameters greatly affects mechanical properties. Therefore, it would be essential to assess the mechanical properties of the actually fabricated wearables for achieving reliable performance although currently, specimens are generally used to test mechanical properties. In addition, it would be beneficial to measure defects in AM wearables by using IR camera, optical tomography, etc. in real time and to reduce failures in final products with closed loop control technology using AI techniques.

Regular audits to operators

Above all, the role of operators or users can be crucial in AM until the application of smart manufacturing, and formal operator certification for the process and material handling is necessary. It may also be necessary to verify the operational stages from time to time through regular audits (AMSC 2018). Conflicts between material savings and increased strength are present in AM, which also affects build time and subsequently, compromises are inevitable (Zhang et al. 2015). However, users can set the parameters, considering performance, material consumption, and build time (Eiliat & Urbanic 2019), and, as a result, lead time can be shortened. Therefore, a win–win situation for both performance of wearables and environmental impact might be achieved if users set the parameters based on an understanding of each AM process parameter and its environmental impact. Logistics practice in Figs. 1 and 2 focuses on most influential AM process parameters on performance of AM wearables affected by user behavior and suggests fabrication constraints related to the parameters. In this respect, the logistics practice differs from other previous studies which deal with just a few process parameters such as the number of parts on the build bed, the gap between the parts etc. (Kadkhoda-Ahmadi et al. 2019) or broad domains such as AM materials, processes, and machines (Zaman et al. 2018).

Identification of specific AM fabrication methods depending on 3D printers

When a human–machine interface system is developed, it must include the ability to present precisely the results for the settings of parameters. To implement this, each AM process must specify an AM fabrication method that includes all parameters related to the quality of the final parts. Furthermore, it is not easy to compare the performance of the output from various 3D printers because the performance and materials of each printer requires particular materials and has different specification. Therefore, it is

important to identify the unique performance of wearables, such as different mechanical properties, depending on the operating conditions of 3D printers and the use of other auxiliary equipment. In particular, it will be necessary to define the control factor, correction coefficient, etc. Therefore, one solution to minimize the effect of user behavior on performance of wearables would be to develop standard operating procedures by AM processes, considering the effect of AM process parameters based on empirical research. Furthermore, the human–machine interface system must present the expected results of the environmental impact with each parameter selection. The system can be utilized in the workplace and provide environmentally friendly incentives to operators who make succeed in reducing environmental impact. For instance, the usage of auxiliary equipment for support removal increases resource consumption and lead time, but manually removing support can reduce consumption (Kwon et al. 2020).

Conclusion

This article reviews parameters of AM processes influenced by user behavior with respect to performance required to fabricate AM wearables. When the user sets the parameters, AM wearables with various performance are fabricated. The AM process parameter that affects the surface topography and geometric and mechanical properties is commonly called part orientation, but its effect appears differently. In particular, the difference in tensile strength has been shown to be more than 40% between part orientations and raster angle and build slope affect mechanical properties and surface topography, respectively. In addition, the effect of some parameters of AM processes can be offset by the type of postprocess, and the outcome of chemical treatment is affected by not the degree of layer thickness but part orientation. The chemical treatment provides the advantages of surface topography but has the disadvantages of some mechanical properties. Therefore, specific effects, such as the order of parameters for each AM process, can be confirmed by performance evaluations performed by setting various parameters, further increasing production reliability (Fig. 2). Especially, when determining the process parameters for wearables, it would be desirable to consider part orientation, build slope, shell thickness and post treatment, although they should be considered for the purpose of the wearable being manufactured.

Current human–machine interface systems have been developed to make it easy to use for users, but they have large limitations in terms of wider application of a feature-based-approach. Due to that, users are currently required to build extensive knowledge of AM technology before fabricating AM parts. Therefore, it is necessary to develop a qualified procedure and to build a database of each AM machine about performance of wearables to minimize the effect of user behavior. The database can be utilized for the development of a human–machine interface system with sophisticated functionality. The database should be built based on the comprehensive experimental design which deals with all parameters of AM processes. Furthermore, each organization can build a database for specific domains that require serial production and multiple parts, and this activity allows them to retain their organization's capabilities.

Most research on the environmental sustainability of AM deals with the resource consumption, so future research will look at resource flow according to parameters of AM processes, and will suggest work practices for the setting of parameters that affect

environmental impact. It is also necessary to develop models for resource consumption evaluation based on the setup of various parameters. Furthermore, a strategy for the improvement of cost efficiency in the AM industry can be established based on resources consumption and AM process parameters.

Abbreviations
AFO: Ankle foot orthosis; AM: Additive manufacturing; FDM: Fused deposition modelling; HIPS: Polystyrene; LS: Laser sintering; PA12: Polyamide12; PJ: Photopolymer jetting; PLA: Polylactic acid; PPE: Personal protective equipment; SL: Laser sintering.

Acknowledgements
Not applicable.

Authors' contributions
JK conceptualized the entire research and design, and drafted the manuscript. NK conceptualized the entire research and design. Both authors read and approved the final manuscript.

Funding
This study is funded by by Ulsan Metropolitan City and the Ministry of Trade, Industry and Energy, Republic of Korea (Project: AM-based eco-friendly auto parts R&BD).

Authors' information
Juyoun Kwon is a Research Professor at the Seoul National University. Namhun Kim is a Professor at the Ulsan National Institute of Science and Technology.

Competing interests
The authors declare that they have no competing interests.

Author details
[1] Research Institute of Human Ecology, Seoul National University, Seoul, Korea. [2] Department of Mechanical Engineering, Ulsan National Institute of Science and Technology, Ulsan, Korea.

Received: 23 September 2020 Accepted: 4 February 2021
Published online: 25 June 2021

References

Afrose, M. F., Masood, S. H., Iovenitti, P., Nikzad, M., & Sharski, I. (2016). Effects of part build orientations on fatigue behaviour of FDM-processed PLA material. *Progress in Additive Manufacturing, 1,* 21–28.
Alharbi, N., Osman, R., & Wismeijer, D. (2016). Effects of build direction on the mechanical properties of 3D-printed complete coverage interim dental restorations. *The Journal of Prosthetic Dentistry, 115,* 760–767.
Ali, M. H., Abilgaziyev, A., & Adair, D. (2019). 4D printing: a critical review of current developments, and future prospects. *The International Journal of Advanced Manufacturing Technology, 105,* 701–717.
Amorim, F. L., Lohrengel, A., Neubert, V., Higa, C. F., & Czelusniak, T. (2014). Selective laser sintering of Mo–CuNi composite to be used as EDM electrode. *Rapid Prototyping Journal, 20,* 59–68.
AMSC. (2017). Standardization roadmap for additive manufacturing. America makes & ANSI. Retrieved September 12, 2020, from https://share.ansi.org/Shared%20Documents/Standards%20Activities/AMSC/AMSC_Roadmap_February_2017.pdf.
Ang, B. Y., Chua, C. K., & Du, Z. H. (2000). Study of trapped material in rapid prototyping parts. *International Journal of Advanced Manufacturing Technology, 16,* 120–130.
Aydin, L., & Kucuk, S. (2018). A method for more accurate FEA results on a medical device developed by 3D technologies. *Polymers Advanced Technologies, 29,* 2281–2286.
Bahr, F., & Westkamper, E. (2018). Correlations between influencing parameters and quality properties of components produced by fused deposition modeling. *Procedia CIRP, 72,* 1214–1219.
Banga, H. K., Belokar, R. M., & Kalra, P. (2018). Fabrication and stress analysis of ankle foot orthosis with additive manufacturing. *Rapid Prototyping Journal, 24*(2), 301–312.
Barbero, E. J. (2011). *Introduction to composite materials design* (2nd ed.). Taylor & Francis Group: CRC Press.
Barclift, M. W., & Williams, C. B. (2012). Examining variability in the mechanical properties of parts manufactured via Polyjet Direct 3D Printing. In *Proceedings of international solid freeform fabrication symposium* (pp. 876–890).
Bates, S. R. G., Farrow, I. R., & Trask, R. S. (2016). 3D printed polyurethane honeycombs for repeated tailored energy absorption. *Materials and Design, 112,* 172–183.
Booth, J. W., Alperovich, J., Chawla, P., Ma, J., Reid, T. N., & Ramani, K. (2017). The design for additive manufacturing worksheet. *Journal of Mechanical Design, 139,* 100904-1–9.
Boschetto, A., & Bottini, L. (2015). Surface improvement of fused deposition modeling parts by barrel finishing. *Rapid Prototyping Journal, 21,* 686–696.
Boschetto, A., Bottini, L., & Veniali, F. (2016). Finishing of fused deposition modeling parts by CNC machining. *Robotics and Computer-Integrated Manufacturing, 41,* 92–101.

Brennan-Craddock, J. P. J., Bingham, G. A., Hague, R. J. M., Wildman, R. D. (2008). Impact absorbent rapid manufactured structures (IARMS). In: *Solid freeform fabrication symposium, Austin, Texas, USA*, August 4–6, 2008 (pp. 266–277).
Burfoot, A. (2019, October 18). Those superfast Nike shoes are creating a problem. *The New York Times.* https://www.nytimes.com/2019/10/18/sports/marathon-running-nike-vaporfly-shoes.html.
Cazon-Martin, A., Iturrizaga-Campelo, M., Matey-Munoz, L., Rodriguez-Ferradas, M. I., Morer-Camo, P., & Ausejo-Munoz, S. (2019). Design and manufacturing of shin pads with multi-material additive manufactured features for football players: A comparison with commercial shin pads. *Proceedings of IMechE Part P: Journal of Sports Engineering and Technology, 233,* 160–169.
Cha, Y. H., Lee, K. H., Ryu, H. J., Joo, I. W., Seo, A., Kim, D. H., & Kim, S. J. (2017). Ankle-foot orthosis made by 3D printing technique and automated design software. *Applied Bionics and Biomechanics, 2017,* 9610468.
Chen, Y. F., Wang, Y. H., & Tsai, J. C. (2019). Enhancement of surface reflectivity of fused deposition modeling parts by post-processing. *Optics Communications, 430,* 479–485.
Chohan, J. S., Singh, R., & Boparai, K. S. (2016). Parametric optimization of fused deposition modeling and vapour smoothing processes for surface finishing of biomedical implant replica. *Measurement, 94,* 602–613.
Choi, H., Peters, K. M., MacConnell, M. B., Ly, K. K., Eckert, E. S., & Steele, K. M. (2017). Impact of ankle foot orthosis stiffness on Achilles tendon and gastrocnemius function during unimpaired gait. *Journal of Biomechanics, 64,* 145–152.
Comina, G., Suska, A., & Filippini, D. (2014). Low cost lab-on-a-chip prototyping with a consumer grade 3D printer. *Lab on a Chip, 14,* 2978.
Comotti, C., Regazzoni, D., Rizzi, C., & Vitali, A. (2017). Additive manufacturing to advance functional design: An application in the medical field. *Journal of Computing and Information Science in Engineering, 17,* 031006–031006–031009.
Corcione, C. E., Greco, A., & Maffezzoli, A. (2006). Temperature evolution during stereolithography building with a commercial epoxy resin. *Polymer Engineering & Science, 46*(4), 493–502.
Cox, S. C., Thornby, J. A., Gibbons, G. J., Williams, M. A., & Mallick, K. K. (2015). 3D printing of porous hydroxyapatite scaffolds intended for use in bone tissue engineering applications. *Materials Science and Engineering C, 47,* 237–247.
Craik, D. J., & Miller, B. F. (1958). The flow properties of powders under humid conditions. *Journal of Pharmacy and Pharmacology, 10*(S1), 136T-T144.
Croccolo, E., De Agostinis, M., & Olmi, G. (2013). Experimental characterization and analytical modelling of the mechanical behaviour of fused deposition processed parts made of ABS-M30. *Computational Materials Science, 79,* 506–518.
Das, S. C., Ranganathan, R., & Murugan, N. (2018). Effect of build orientation on the strength and cost of Polyjet 3D printed parts. *Rapid Prototyping Journal, 24,* 832–839.
Davia-Aracil, M., Hinojo-Perez, J. J., Jimeno-Morenilla, A., & Mora-Mora, H. (2018). 3D printing of functional anatomical insoles. *Computers in Industry, 95,* 38–53.
Dawoud, M., Tha, I., & Ebeid, S. J. (2016). Mechanical behaviour of ABS: An experimental study using FDM and injection moulding techniques. *Journal of Manufacturing Processes, 21,* 39–45.
Deckers, J. P., Vermandel, M., Geldhof, J., Vasiliauskaite, E., Forward, M., & Plasschaert, F. (2018). Development and clinical evaluation of laser-sintered ankle foot orthoses. *Plastics, Rubber and Composites, 47*, 42–46.
DNV GL. (2017). Additive manufacturing-qualification and certification process for materials and components. DNV GL AS. DNVGL-CG-0197. Retrieved September 12, 2020, from https://rules.dnvgl.com/docs/pdf/DNVGL/CG/2017-11/DNVGL-CG-0197.pdf.
Ebel, E., & Sinnemann, T. (2014). Fabrication of FDM 3D objects with ABS and PLA determination of their mechanical properties. *RTejournal*. Retrieved September 12, 2020, from https://www.rtejournal.de/ausgabe11/3872.
Ebert, J., Ozkoi, E., Zeicher, A., Uibel, K., Weiss, O., Koops, U., et al. (2009). Direct inkjet printing of dental prostheses made of zirconia. *Journal of Dental Research, 88,* 673–676.
Eiliat, H., & Urbanic, J. (2019). Determining the relationships between the build orientation, process parameters and voids in additive manufacturing material extrusion processes. *International Journal of Advanced Manufacturing Technology, 100,* 683–705.
Eshraghi, S., & Das, S. (2010). Mechanical and microstructural properties of polycaprolactone scaffolds with 1-D, 2-D, and 3-D orthogonally oriented porous architectures produced by selective laser sintering. *Acta Biomaterialia, 6,* 2467–2476.
Es-Said, O. S., Foyos, J., Noorani, R., Mendelson, M., Marloth, R., & Pregger, B. A. (2000). Effect of layer orientation on mechanical properties of rapid prototyped samples. *Materials and Manufacturing Processes, 15,* 107–122.
Faludi, J., Bayley, C., Bhogal, S., & Iribarne, M. (2015). Comparing environmental impacts of additive manufacturing vs traditional machining via life-cycle assessment. *Rapid Prototyping Journal, 21,* 14–33.
Faustini, M. C., Neptune, R. R., Crawford, R. H., & Stanhope, S. J. (2008). Manufacture of passive dynamic ankle-foot orthoses using selective laser sintering. *IEEE Transaction Biomedicine Engineering, 55,* 784–790.
FDA. (1997). Design control guidance for medical device manufacturers. FDA. Retrieved September 12, 2020, from https://www.fda.gov/regulatory-information/search-fda-guidance-documents/design-control-guidance-medical-device-manufacturers.
Fierz, F. C., Beckmann, F., Huser, M., Irsen, S. H., Leukers, B., Witte, F., et al. (2008). The morphology of anisotropic 3D-printed hydroxyapatite scaffolds. *Biomaterials, 2,* 3799–3806.
Fulcher, B., & Leigh, D. K. (2012). Effect of segregated first and second melt point on laser sintered part quality and processing. In *Proceedings of the 23rd international solid freeform fabrication symposium*.
Galantucci, L. M., Lavecchia, F., & Percoco, G. (2009). Experimental study aiming to enhance the surface finish of fused deposition modeled parts. *CIRP Annals Manufacturing Technology, 58,* 189–192.
Galantucci, L. M., Lavecchia, F., & Percoco, G. (2010). Quantitative analysis of a chemical treatment to reduce roughness of parts fabricated using fused deposition modeling. *CIRP Annals Manufacturing Technology, 51*, 247–250.
Garg, A., Bhattacharya, A., & Batish, A. (2016). On surface finish and dimensional accuracy of FDM parts after cold vapor treatment. *Materials and Manufacturing Processes, 31,* 522–529.

Garg, A., Bhattacharya, A., & Batish, A. (2017). Chemical vapor treatment of ABS parts built by FDM: Analysis of surface finish and mechanical strength. *International Journal of Advanced Manufacturing Technology, 89,* 2175–2191.
Gibson, I., & Shi, M. (1997). Material properties and fabrication parameters in selective laser sintering process. *Rapid Prototyping Journal, 3,* 129–136.
GrabCad. (2019). Adjusting print settings. Retrieved September 12, 2020, from https://help.grabcad.com/article/226-adjusting-print-settings?locale=ko.
Guan, H. W., Savalani, M. M., Gibson, I., & Diegel, O. (2015). Influence of fill gap on flexural strength of parts fabricated by curved layer fused deposition modeling. *Procedia Technology, 20,* 243–248.
Guerra, M. G., Volpone, C., Galantucci, L. M., & Percoco, G. (2018). Photogrammetric measurements of 3D printed microfluidic devices. *Additive Manufacturing, 21,* 53–62.
Hill, N., & Haghi, M. (2014). Deposition direction-dependent failure criteria for fused deposition modelling polycarbonate. *Rapid Prototyping Journal, 20,* 221–227.
Huang, B., Meng, S., He, H., Jia, Y., Xu, Y., & Huang, H. (2019). Study of processing parameters in fused deposition modeling based on mechanical properties of acrylonitrile-butadiene-styrene filaments. *Polymer Engineering and Science*. https://doi.org/10.1002/pen.24875.
Huang, B., & Singamneni, S. (2015). Raster angle mechanics in fused deposition modelling. *Journal of Composite Materials, 49,* 363–383.
Ielapi, A., Lammens, N., Paepegem, W. V., Forward, M., Deckers, J. P., Vermandel, M., & Beule, M. D. (2019). A validated computational framework to evaluate the stiffness of 3D printed ankle foot orthoses. *Computer Methods in Biomechanics and Biomedical Engineering, 22*(8), 880–887.
ISO/ASTM 52921:2013. (2016). *Standard terminology for additive manufacturing-coordinate systems and test methodologies*. West Conshohocken: ASTM.
Ituarte, I. F., Boddeti, N., Hassani, V., Dunn, M. L., & Rosen, D. W. (2019). Design and additive manufacture of functionally graded structures based on digital materials. *Additive Manufacturing, 30,* 100839.
Jin, Y., He, Y., & Shih, A. (2016). Process planning for the fused deposition modeling of ankle-foot-orthoses. *Procedia CIRP, 42*, 760–765.
Johnson, A., Bingham, G. A., & Wimpenny, D. I. (2013). Additive manufactured textiles for high-performance stab resistant applications. *Rapid Prototyping Journal, 19,* 199–207.
Kadkhoda-Ahmadi, S., Hassan, A., & Asadollahi-Yazdi, E. (2019). Process and resource selection methodology in design for additive manufacturing. *The International Journal of Advanced Manufacturing Technology, 104,* 2013–2029.
Kesy, A., & Kotlinski, J. (2010). Mechanical properties of parts produced by using polymer jetting technology. *Archives of Civil and Mechanical Engineering, 3,* 37–50.
Khoshkhoo, A., Carrano, A. L., & Blersch, D. M. (2018). Effect of surface slope and build orientation on surface finish and dimensional accuracy in material jetting processes. *Procedia Manufacturing, 26,* 720–730.
Kim, H., Lin, Y., & Tseng, T. L. B. (2018). A review on quality control in additive manufacturing. *Rapid Prototyping Journal, 24,* 645–669.
Kim, G. D., & Oh, Y. T. (2008). A benchmark study on rapid prototyping processes and machines: Quantitative comparisons of mechanical properties, accuracy, roughness, speed, and material cost. *Proceedings of IMechE: Journal of Engineering and Manufacture, 222,* 201–215.
Kollmuss, A., & Agyeman, J. (2002). Mind the Gap: Why do people act environmentally and what are the barriers to pro-environmental behaviour? *Environmental Education Research, 8*(3), 239–260.
Kozior, T., Dopke, C., Crimmelsmann, N., Junger, I. J., & Ehrmann, A. (2018). Influence of fabric pretreatment on adhesion of three-dimensional printed material on textile substrates. *Advances in Mechanical Engineering, 10*(8), 1–8.
Kuo, C., & Mao, R. (2016). Development of a precision surface polishing system for parts fabricated by fused deposition modeling. *Materials and Manufacturing Processes, 31*(8), 1113–1118.
Kuo, C. C., & Su, S. J. (2013). A simple method for improving surface quality of rapid prototype. *Indian Journal of Engineering & Materials Sciences, 20,* 465–470.
Kwon, J., Kim, N., & Ma, J. (2020). Environmental sustainability evaluation of additive manufacturing using the NIST test artifact. *Journal of Mechanical Science and Technology, 34*(3), 1265–1274.
Kwon, J., Park, H. Y., Park, Y. B., & Kim, N. (2017). Potentials of additive manufacturing with smart materials for chemical biomarkers in wearable applications. *International Journal of Precision Engineering and Manufacturing-Green Technology, 4,* 335–347.
Lalehpour, A., & Barari, A. (2016). Post processing for fused deposition modeling parts with acetone vapour bath. *IFAC-PapersOnLine, 49–31,* 42–48.
Lanzotti, A., Grasso, M., Staiano, G., & Martorelli, M. (2015). The impact of process parameters on mechanical properties of parts fabricated in PLA with an open-source 3-D printer. *Rapid Prototyping Journal, 21,* 604–617.
Lee, C. S., Kim, S. G., Kim, H. J., & Ahn, S. H. (2007). Measurement of anisotropic compressive strength of rapid prototyping parts. *Journal of Materials Processing Technology, 187–188,* 627–630.
Li, H., Wang, T., & Yu, Z. (2017). The quantitative research of interaction between key parameters and the effects on mechanical property in FDM. *Advances in Materials Science and Engineering, 2017,* 9152954.
Liu, W., Zhu, Z., & Ye, S. (2019). Industrial case studies of design for plastic additive manufacturing for end-use consumer products. *3D Printing and Additive Manufacturing, 2*(6), 281–292.
Lunsford, C., Grindle, G., Salatin, B., & Dicianno, B. E. (2016). Innovations with 3-dimensional printing in physical medicine and rehabilitation: A review of the literature. *PM&R, 8,* 1201–1212.
Luzanin, O., Guduric, V., Ristic, I., & Muhic, S. (2017). Investigating impact of five build parameters on the maximum flexural force in FDM specimens—A definitive screening design approach. *Rapid Prototyping Journal, 23,* 1088–1098.
Majewski, C., & Hopkinson, N. (2011). Effect of section thickness and build orientation on tensile properties and material characteristics of laser sintered nylon-12 parts. *Rapid Prototyping Journal, 17,* 176–180.
Mavroidis, C., Ranki, R. G., Sivak, M. L., Patritti, B. L., DiPisa, J., Caddle, A., et al. (2011). Patient specific ankle-foot orthoses using rapid prototyping. *Journal of NeuroEngineering and Rehabilitation, 8*(1), 1–11.

Meisel, N. A., Elliott, A. M., & Williams, C. B. (2015). A procedure for creating actuated joints via embedding shape memory alloys in polyjet 3D printing. *Journal of Intelligent Material Systems and Structures, 26*(12), 1498–1512.
Mercelis, P., & Kruth, J. (2006). Residual stresses in selective laser sintering and selective laser melting. *Rapid Prototyping Journal, 12,* 254–265.
Miclaus, R., Repanovici, A., & Roman, N. (2017). Biomaterials: Polylactic acid and 3D printing processes for orthosis and prosthesis. *Materiale Plastice, 54,* 98–102.
Moges, T., Ameta, G., & Witherell, P. (2019). A review of model inaccuracy and parameter uncertainty in laser powder bed fusion models and simulations. *Journal of Manufacturing Science and Engineering, 141,* 040801-1-040801–14.
Mohan, N., Senthil, P., Vinodh, S., & Jayanth, N. (2017). A review on composite materials and process parameters optimisation for the fused deposition modelling process. *Virtual and Physical Prototyping, 12,* 47–59.
Nancharaiah, T., Raju, D. R., & Raju, V. R. (2010). An experimental investigation on surface quality and dimensional accuracy of FDM component. *International Journal on Emerging Technologies, 1*(2), 106–111.
Pallari, J. H. P., Dalgarno, K. W., & Woodburn, J. (2010). Mass customization of foot orthoses for rheumatoid arthritis using selective laser sintering. *IEEE Transactions on Biomedical Engineering, 57*(7), 1750–1756.
Palousek, D., Rosicky, F., Koutny, D., Stoklask, P., & Navrat, T. (2014). Pilot study of the wrist orthosis design process. *Rapid prototyping journal, 20*(1), 27–32.
Paterson, A. M., Bibb, R., Campbell, R. I., & Bingham, G. (2015). Comparing additive manufacturing technologies for customized wrist splints. *Rapid Prototyping Journal, 21,* 230–243.
Percoco, G., Lavecchia, F., & Galantucci, L. M. (2012). Compressive properties of FDM rapid prototypes treated with a low cost chemical finishing. *Research Journal of Applied Sciences Engineering and Technology., 4*(19), 3838–3842.
Raghunath, N., & Pandey, P. M. (2007). Improving accuracy through shrinkage modelling by using Taguchi method in selective laser sintering. *International Journal of Machine Tools & Manufacture, 47,* 985–995.
Raut, S., Jatti, V. S., Khedkar, N. K., & Singh, T. P. (2014a). Investigation of the effect of build orientation on mechanical properties and total cost of FDM parts. *Procedia Materials Science, 6,* 1625–1630.
Raut, S., Jatti, V. S., & Singh, T. P. (2014b). Influence of built orientation on mechanical properties in fused deposition modeling. *Applied Mechanics and Materials, 592–594,* 400–404.
Rebaioli, L., & Fassi, I. (2017). A review on benchmark artifacts for evaluating the geometrical performance of additive manufacturing processes. *International Journal of Advanced Manufacturing Technology, 93,* 2571–2598.
Rodriguez, J. F., Thomas, J. P., & Renaud, J. E. (2000). Characterization of the mesostructure of fused deposition acrylonitrile-butadiene-styrene materials. *Rapid Prototyping Journal, 6,* 176–185.
Rossiter, J. D., Johnson, A. A., & Bingham, G. A. (2020). Assessing the design and compressive performance of material extruded lattice structures. *3D Printing and Additive Manufacturing, 7*(1), 19–27.
Santos, S., Soares, B., Leite, M., & Jacinto, J. (2017). Design and development of a customized knee positioning orthosis using low cost 3D printers. *Virtual and Physical Prototyping, 12*(4), 322–332.
Scharff, R. B. N., Doubrovski, E. L., Poelman, W. A., Jonker, P. O., Wang, C. C. L., & Geraedits, J. M. P. (2017). Towards behaviour design of a 3D-printed soft robotic hand. *Soft Robotics: Trends Applications and Challenges, 17,* 23–29.
Schrank, E. S., & Stanhope, S. J. (2011). Dimensional accuracy of ankle-foot orthoses constructed by rapid customization and manufacturing framework. *Journal of Rehabilitation Research & Development, 48,* 31–42.
Seo, S. P. (2012). Quantitative analysis on SLS part curling using EOS P770 machine. *Journal of Materials Processing Technology, 212,* 2433–2442.
Silbert, J. (2019, February 25). Nike finally launches vapor fly elite flyprint 3D, restricts sales to marathon runners. *Hypebeast.* https://hypebeast.com/2019/2/nike-vaporfly-elite-flyprint-3d-japan-release-info.
Soe, S. P., Eyers, D. R., & Setchi, R. (2013). Assessment of non-uniform shrinkage in the laser sintering of polymer materials. *International Journal of Advanced Manufacturing Technology, 68,* 111–125.
Soe, S. P., Martin, P., Jones, M., Robinson, M., & Theobald, P. (2015). Feasibility of optimizing bicycle helmet design safety through the use of additive manufactured TPE cellular structures. *International Journal of Advanced Manufacturing Technology., 79,* 1975–1982.
Song, R., & Telenko, C. (2016). Material waste of commercial FDM printers under realistic conditions. In *Proceedings of the 27th annual international solid freeform fabrication symposium 2016: An additive manufacturing conference.*
Song, R., & Telenko, C. (2019). Causes of desktop FDM fabrication failures in an open studio environment. In *Proceedings of 26th CIRP life cycle engineering (LCE) conference: Procedia CIRP* (Vol. 80, pp. 494–499).
Spisak, E., Gajdos, I., & Slota, J. (2014). Optimization of FDM prototypes mechanical properties with path generation strategy. *Applied Mechanics and Materials, 474,* 273–278.
Stansbury, J. W., & Idacavage, M. J. (2016). 3D printing with polymers: Challenges among expanding options and opportunities. *Dental Materials, 32,* 54–64.
Sun, Q., Rizvi, G. M., Bellehumeur, C. T., & Gu, P. (2008). Effect of processing conditions on the bonding quality of FDM polymer filaments. *Rapid Prototyping Journal, 14,* 72–80.
Tao, Y., Shao, J., Li, P., & Shi, S. Q. (2019). Application of a thermoplastic polyurethane/polylactic acid composite filament for 3D-printed personal orthosis. *MTAEC9, 53*(1), 71–76.
Telfer, S., Pallari, J., Munguia, J., Dalgarno, K., McGeough, M., & Woodburn, J. (2012). Embracing additive manufacture: implications for foot and ankle orthosis design. *BMC Musculoskeletal Disorders, 13,* 1471–2474.
Torres, J., Cole, M., Owji, A., DeMastry, Z., & Gordon, A. P. (2016). An approach for mechanical property optimization of fused deposition modelling with polylactic acid via design of experiments. *Rapid Prototyping Journal, 22,* 387–404.
Tseng, T. L. B., Chilukuri, A., Park, S. C., & Kwon, Y. J. (2014). Automated quality characterization of 3D printed bone scaffolds. *Journal of Computational Design and Engineering, 3*(1), 194–201.
Udroiu, R., Braga, I. C., & Nedelcu, A. (2019). Evaluating the quality surface performance of additive manufacturing systems: Methodology and a material jetting case study. *Materials, 12,* 995.
Valtas, A., & Sun, D. (2016). 3D printing for garments production: An exploratory study. *Journal of Fashion Technology & Textile Engineering, 4,* 1000139.
Vasudevarao, B., Natarajan, D. P., & Henderson, M. (2000). Sensitivity of RP surface finish to process parameter variation. *Proceedings of solid freeform fabrication, Austin, TX* (pp. 252–258).

Vidakis, N., Petousis, M., Viris, A., Savvakis, K., & Maniaki, A. (2017). On the compressive behaviour of an FDM Steward Platform part. *Journal of Computational Design and Engineering, 4,* 339–346.
Walbran, M., Turner, K., & McDaid, A. J. (2016). Customized 3D printed ankle-foot orthosis with adaptable carbon fibre composite spring joint. *Cogent Engineering, 3,* 1227022.
Wallin, T. J., Pikul, J., & Shephard, R. F. (2018). 3D printing of soft robotic systems. *Nature, 3,* 84–100.
Wan, H. Y., Chen, G. F., Li, C. P., Qi, X. B., & Zhang, G. P. (2019). Data-driven evaluation of fatigue performance of additive manufactured parts using miniature specimens. *Journal of Materials Processing Technology, 35,* 1137–1146.
Wang, T. M., Xi, J. T., & Jin, Y. (2007). A model research for prototype warp deformation in the FDM process. *International Journal of Advanced Manufacturing Technology, 33,* 1087–1096.
Wang, W. L., Cheah, C. M., Fuh, J. Y. H., & Lu, L. (1996). Influence of process parameters on stereolithography part shrinkage. *Materials & Design, 17*(4), 205–213.
Weiss, K. P., Bagrets, N., Lange, C., Goldacker, W., & Wohlgemuth, J. (2015). Thermal and mechanical properties of selected 3D printed thermoplastics in the cryogenic temperature regime. *IOP Conference Series: Materials Science and Engineering, 102,* 012022.
Wojciechowski, E., Chang, A. Y., Balassone, D., Ford, J., Cheng, T. L., Little, D., et al. (2019). Feasibility of designing, manufacturing and delivering 3D printed ankle-foot orthoses: A systematic review. *BMC Journal of Foot and Ankle Research, 12*(11), 1–12. https://doi.org/10.1186/s13047-019-0321-6.
Xu, F., Loh, H. T., & Wong, Y. S. (1999). Considerations and selection of optimal orientation for different rapid prototyping systems. *Rapid Prototyping Journal, 5,* 54–60.
Yan, C., Shi, Y., Yang, J., & Liu, J. (2010). Multiphase polymeric materials for rapid prototyping and tooling technologies and their application. *Composite Interfaces, 17,* 257–271.
Yang, S., & Evans, J. R. G. (2007). Metering and dispensing of powder; the quest for new solid freeforming techniques. *Powder Technology, 178,* 56–72.
Yang, J. H., Zhao, Z. J., & Park, S. H. (2015). Evaluation of directional mechanical properties of 3D printed polymer parts. In *Proceedings of the 15th international conference on control, automation and systems*.
Yao, X., Moon, S. K., & Bi, G. (2017). Multidisciplinary design optimization to identify additive manufacturing resources in customized product development. *Journal of Computational Design and Engineering, 4,* 131–142.
Yarwindran, M., Azwani Sa'aban, N., Ibrahim, M., & Raveverma, P. (2016). Thermoplastic elastomer infill pattern impact on mechanical properties 3D printed customized orthotic insole. *ARPN Journal of Engineering and Applied Sciences, 11,* 6519–6524.
Yeo, K. J. C., & Lim, C. T. (2016). Emerging flexible and wearable physical sensing platforms for healthcare and biomedical applications. *Microsystems & Nanoengineering, 2,* 160403.
Zaman, U. K., Rivette, M., Siadat, A., & Mousavi, S. M. (2018). Integrated product-process design: Material and manufacturing process selection for additive manufacturing using multi-criteria decision making. *Robotics and Computer-Integrated Manufacturing, 51,* 169–180.
Zarringhalam, H., Hopkinson, N., Kamperman, N. F., & de Vlieger, J. J. (2006). Effects of processing on microstructure and properties of SLS Nylon 12. *Materials Science and Engineering A, 435–436,* 172–180.
Zehtaban, L., Elazhary, O., & Roller, D. (2016). A framework for similarity recognition of CAD models. *Journal of Computational Design and Engineering, 3,* 274–285.
Zhang, X., Chen, L., Mulholland, T., & Osswald, T. A. (2019). Effects of raster angle on the mechanical properties of PLA and AL/PLA composite part produced by fused deposition modeling. *Polymers Advanced Technologies, 30,* 2122–2135.
Zhang, X., Xia, Y., Wang, J., Yang, Z., Tu, C., & Wang, W. (2015). Medial axis tree-an internal supporting structure for 3D printing. *Computer Aided Geometric Design, 35–36,* 149–162.
Zhang, Y. C., Bernard, A., Gupta, R. K., & Harik, R. (2016). Feature based building orientation optimization for additive manufacturing. *Rapid Prototyping Journal, 22,* 358–376.

Publisher's Note